

DROP SHAPE AND DSD RETRIEVAL WITH AN X-BAND DUAL POLARIZATION RADAR

E. Gorgucci*, L. Baldini, Institute of Atmospheric Sciences and Climate – CNR, Rome, Italy
 V. Chandrasekar, Colorado State University, Fort Collins CO 80523

1. INTRODUCTION

There is a renewed interest in the use of X-band weather radars, due to specific advantages such as applications to rainfall estimation in light rain, monitoring of sensitive areas that are inadequately covered by operational radar networks as well as the radar network concept introduced by the Center for Collaborative Adaptive Sensing of the Atmosphere (CASA) (Chandrasekar et al. 2004). The use of X-band measurements has been made easier by the advances in attenuation correction techniques based on polarimetric measurements. The initial set of attenuation correction algorithms was built from differential propagation phase (Φ_{dp}) (Bringi et al. 1991). Among the new algorithms that have been proposed, one of the most popular is that of Testud et al. (2000), that adopts a final value constraint as used in space borne radar. One of the advantages of polarimetric radar measurements is the internal self-consistency (Scarchilli et al. 1996), that expresses the synergy of the radar measurements of reflectivity factor (Z_h), differential reflectivity (Z_{dr}), and specific differential phase (K_{dp}). Recently, it has been employed in a technique for attenuation and differential attenuation correction (Gorgucci et al. 2006a; Gorgucci and Baldini 2007). The technique, enforcing self-consistency between K_{dp} , and corrected Z_h and Z_{dr} measurements, improves the estimate provided by the methods that use Φ_{dp} as a constraint.

Many studies on dual polarization radars have shown that observations at S-band can be used to derive raindrop size distribution parameters (Gorgucci et al. 2002; Bringi et al. 2003; Brandes et al. 2003) and mean raindrop shape (Gorgucci et al. 2000; Moisseev et al. 2006; Gorgucci et al. 2006b). This paper takes the next steps, namely the retrieval of drop shape and drop size distribution parameters using attenuation corrected polarimetric radar measurements at X-band.

2. RAIN MICROPHYSICS

The drop size distribution (DSD) describes the probability density distribution function of raindrop sizes. A gamma distribution model has been shown to adequately describe many of the natural variations in

the shape of the raindrop size distribution (Ulbrich 1983). To compare the probability density function of D in the presence of varying water contents, the concept of scaling the DSD has been used by several authors (Illingworth and Blackman 2002). The corresponding form of the DSD can be expressed as

$$N(D) = N_w f(\mu) \left(\frac{D}{D_0} \right)^\mu \exp \left[- (3.67 + \mu) \frac{D}{D_0} \right] \quad (1)$$

where $f(\mu)$ is a dimensionless function of μ given by

$$f(\mu) = \frac{6}{(3.67)^4} \cdot \frac{(3.67 + \mu)^{\mu+4}}{\Gamma(\mu + 4)} \quad (2)$$

with $f(0)=1$. One interpretation of N_w is that it is the intercept of an equivalent exponential distribution with the same water content. D_0 is the median volume diameter and μ is the shape factor of the gamma DSD.

Wind tunnel measurements, observations with 2D video disdrometers as well as airborne 2D probes indicate that the shape of raindrops can be approximated by oblate spheroids described by semimajor axis a and semiminor axis b . The relationship of the axis ratio $r=b/a$ with drop diameter can be approximated by (Gorgucci et al. 2000)

$$r(D) = 1.03 - \beta D \quad (3)$$

with $r=1$ when $D \leq 0.03/\beta$. The linear fit to the wind tunnel data of Pruppacher and Beard (1970) corresponds to $\beta=0.062 \text{ mm}^{-1}$ (the drop-shape model corresponding to this value of β will be henceforth referred to as PB). If the mean axis ratio versus D relation is nonlinear, it is always possible to define a linear relation that results in the same K_{dp} (Bringi et al. 2003).

3. POLARIMETRIC RADAR RETRIEVAL OF DROP SHAPE AND DSD PARAMETERS

Seliga et al. (1981) showed that the two parameters of an exponential DSD can be estimated from Z_h and Z_{dr} assuming an equilibrium raindrop shape model. This procedure can be generalized for a normalized gamma DSD and a generic drop-shape model.

Gorgucci et al. (2006b) pointed out that collapsing the self-consistency principle onto a two-dimensional space defined by the two variables K_{dp}/Z_h and Z_{dr} , the influence of DSD is nullified so that the drop shape variability can be observed. At S-band, they used this approach to infer the prevailing shape of the raindrops

* Corresponding author address: Eugenio Gorgucci, ISAC-CNR, Via Fosso del Cavaliere, 100, 00133 Roma, Italy; e-mail: e.gorgucci@isac.cnr.it

along the path directly from polarimetric radar measurements. This result suggests to replace the β retrieval algorithm in Gorgucci et al. (2000) with a function of the two variables K_{dp}/Z_h and Z_{dr} , of the form

$$\beta_e = c_1 \left(\frac{K_{dp}}{Z_h} \right)^{a_1} \xi_{dr}^{b_1} \quad (4)$$

where ξ_{dr} is the dimensionless differential reflectivity defined by $Z_{dr}=10\log_{10}\xi_{dr}$, and Z_h is in $\text{mm}^6 \text{m}^{-3}$.

Gorgucci et al. (2002) showed that gamma DSD parameters can be estimated through relationships whose coefficients depend on β . Therefore, once β is estimated from (4), a parameterization for D_0 and N_w can be pursued of the form

$$D_0 = c_2 \left(\frac{\xi_{dr} - 0.8}{\beta} \right)^{a_2} \quad (5)$$

$$\log_{10} N_w = c_3 \left(\frac{\xi_{dr} - 0.8}{\beta} \right)^{a_3} Z_h^{b_3} \quad (6)$$

where N_w is given in $\text{mm}^{-1} \text{m}^{-3}$. Coefficients of (5) and (6) can be estimated through simulation. A large number of gamma DSDs (100000 triplets) are simulated, varying the parameters of (1) in a wide range ($0.5 < D_0 < 3.5 \text{ mm}$, $3 < \log_{10} N_w < 5$, and $-1 < \mu < 5$), and using the constraints of $10\log_{10} Z_h < 55 \text{ dBZ}$ and rainfall rate less than 300 mm h^{-1} (Bringi and Chandrasekar 2001). Under these conditions, Z_h , Z_{dr} , and K_{dp} measurements are simulated at a temperature of 20°C , and assuming the shape-size model (3) with β ranging from 0.04 to 0.08 mm^{-1} . A nonlinear regression analysis is then performed to estimate the coefficients of (4), (5) and (6). Coefficients for X-band (9.3 GHz) are: $c_1=0.536$, $a_1=0.276$, and $b_1=1.212$; $c_2=0.201$, $a_2=0.884$; $c_3=7.030$, $a_3=-0.581$, $b_3=0.083$. The parameterization of D_0 is characterized by a normalized bias (NB) of 0.6% and a normalized standard error (NSE) of 12% , whereas NB and NSE of (5) are -0.3% and 7% , respectively. NB and NSE are defined as the difference between the mean estimated and true values normalized to the mean true value, and the root mean square error normalized with respect to the mean true value, respectively.

5. SIMULATION AND ANALYSIS

Attenuation and differential attenuation will result in errors in the microphysical estimates obtained using (4), (5) and (6). However, also errors in attenuation correction will have an impact in the retrieved β , D_0 , and N_w . To evaluate this impact, it would be necessary knowing rain microphysics in each radar bin. Since this is not realistic, we need to perform this analysis using

simulation. For this purpose, X-band (9.3 GHz) range profiles generated from S-band (3 GHz) observations using the technique by Chandrasekar et al. (2006) can be used. Assuming a drop-shape model and using the self-consistency principle, for each bin of a measured S-band rain profile, a DSD that generates radar measurements equal to those measured in the same bin is assigned. In this way, DSD profiles are obtained and can be used to generate X-band profiles of unattenuated Z_h and Z_{dr} , and K_{dp} . Corresponding profiles of the attenuation and differential attenuation at X-band can be also generated to obtain Z_h and Z_{dr} attenuated profiles.

The S-band radar data used for this simulation were collected by the NCAR S-Pol radar during the Texas Florida Underflight Experiment (TEFLUN-B). Test data were obtained selecting rain profiles of 15-km length (100 range bins with a 0.150-km resolution in range) that presents at least 3 degrees of increase in Φ_{dp} . A set of 6400 profiles was selected. Signal fluctuation and differential phase on backscattering are also included in the simulated X-band profiles. In particular, signal random fluctuation is generated (Chandrasekar and Bringi 1987) in such a way that Z_h , Z_{dr} , and Φ_{dp} measurement errors correspond to 1 dB, 0.3 dB, and 3 degrees, respectively. In this way, two sets of X-band profiles, composed of "true" (non attenuated) and "measured" (attenuated) profiles are obtained.

Attenuation and differential attenuation correction of "measured" profiles are performed here using the fully self consistent method (FSC) described in Gorgucci and Baldini (2007) with coefficients for X-band built based on the same DSD data set described in the previous section and assuming β to vary between 0.04 and 0.08 mm^{-1} . In this way, the parameterizations will result optimized for varying drop shape. A third set, consisting of "FSC" corrected profiles is obtained correcting for attenuation and differential attenuation the "measured" profiles.

For each path, a value of β is estimated by (4) computing Z_h from the mean power along the path, ξ_{dr} as the ratio between the mean powers at h and v polarizations, and K_{dp} as the mean value obtained from the finite difference between the values at the end and at the beginning of the of Φ_{dp} profile. Conversely, D_0 and N_w are computed, using (5) and (6), respectively, in each range bin.

The performances of the retrieval algorithms are studied first using 15-km radar profiles generated assuming drops following the PB model.

The estimation of β is affected by Z_h , Z_{dr} and K_{dp} measurement errors. Moreover, having Z_h and Z_{dr} to be corrected for attenuation and differential attenuation, inaccuracies of the correction procedure will directly translate into errors of β estimate. This parameter was computed using the three data sets described before.

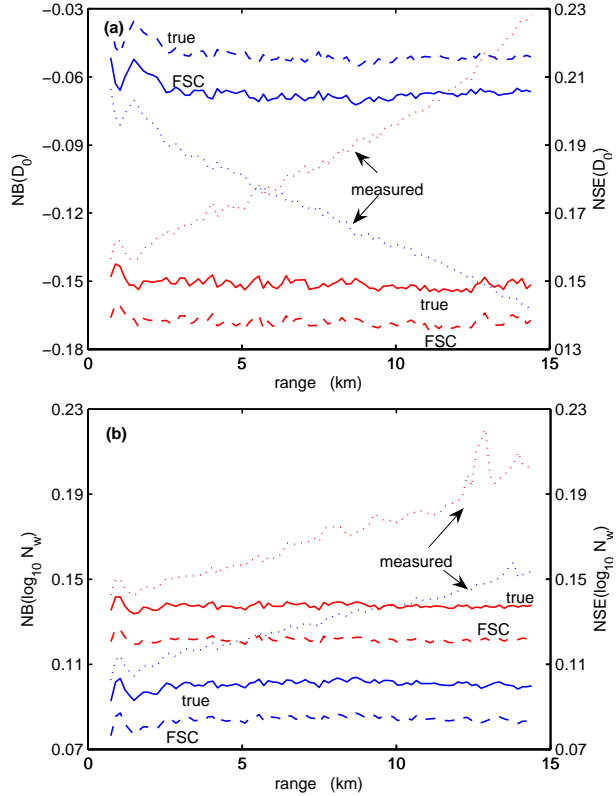


Fig. 1: NB (blue) and NSE (red) of (a) D_0 and (b) $\log_{10}(N_w)$ estimated using (5) and (6), respectively, with true (dashed line), measured (dotted line) and FSC corrected (solid line) profiles as a function of range. Rain drops along the path follow the PB drop shape model.

The NB and NSE of β computed with the “true” data set are 3.4 and 5.1%, respectively, and represent the accuracy of the parameterization (4). If “attenuated” profiles are used, NB and NSE slightly increase up to 5.3 and 7.7%, respectively. In fact, β estimated with attenuated Z_h and Z_{dr} is not too much affected by attenuation, due to a compensation between attenuation and differential attenuation in (4). The FSC technique introduces a correction that bring back the NB to a value (3.4 %) comparable to of the “true” profiles, and reduces the NSE to 6.5 %.

Fig. 1a shows NB (blue) and NSE(red) of D_0 estimated with (5), using “true” (dashed line), “attenuated” (dotted line) and “FSC” corrected profiles (solid line) as a function of range. The very good performance of D_0 estimation is pointed out by the very small difference between the values obtained using true and FSC corrected profiles, about 1% and 2% for NB and NSE, respectively. This result is primarily due to the goodness of the attenuation correction procedure, since

differences between the “true” and “FSC” corrected lines are only due to the attenuation correction procedure, whereas NB and NSE obtained using the “true” profiles give a weight of the accuracy of the parameterization. Moreover, it has to be pointed out that the evident increase of NB and NSE with the range obtained using attenuated values is totally removed by the FSC correction technique. Fig. 1b shows the results for the retrieval of $\log_{10}N_w$. Also in this case, the very good performance of (6) is highlighted by the small difference, both in NB and NSE, between the values obtained using true and FSC corrected profiles.

Analyzing radar data collected by the NCAR S-POL radar in Florida during 1999, Gorgucci et al. (2006b) showed that the drop shape retrieved from polarimetric radar data presents a variability bordered between the PB model and the equilibrium model of Beard and Chuang (1987), henceforth referred to as BC. For this reason, the retrieval procedure is also analyzed in the presence of a rain medium whose raindrops follow the BC shape-size model. In this way, it is possible to verify the ability of β to represent a non linear drop shape model like the BC.

Results are shown in Fig. 2 where NB (blue) and NSE (red) of D_0 (Fig. 2a) and $\log_{10}N_w$ (Fig. 2v) estimates are shown as a function of the range for the three sets of “true” (dashed line), “attenuated” (dotted line) and “FSC corrected” profiles (solid line). The merit factors indicate performances similar to those obtained with drops following the PB drop shape model shown in Fig. 1. The effect related to the use of an equivalent linear relation for the drop shape can be seen analyzing the lines of the “true” profiles. In particular, the estimation of D_0 presents a variation of about 2% and 1% in the NB and NSE, respectively. In the estimation of $\log_{10}N_w$, both NB and NSE present negligible variations with respect to the case of profiles generated assuming the PB drop-shape model. Regarding the attenuation correction, it can be seen that FSC lines show a variation of about 1% with respect to corresponding lines in Fig. 1, with the exception of the NB of D_0 that remains unchanged.

6. EXPERIMENTAL RESULTS

To study the retrieval techniques with measured X-band radar profiles, polarimetric radar measurements collected by the NOAA ESRL X-band transportable polarimetric radar (Martner et al. 2001) during the field campaign conducted by Dr. C. Kummerow at the NASA Wallops Island facility in Virginia are used. Measurements were collected using a scheme based on the transmission of a slanted 45° linear polarization and on the simultaneous reception of echoes at horizontal and vertical polarizations by means of two linear receivers (Matrosov et al. 2002). The data refer to a rain event that took place on 11 April 2001 between 1515

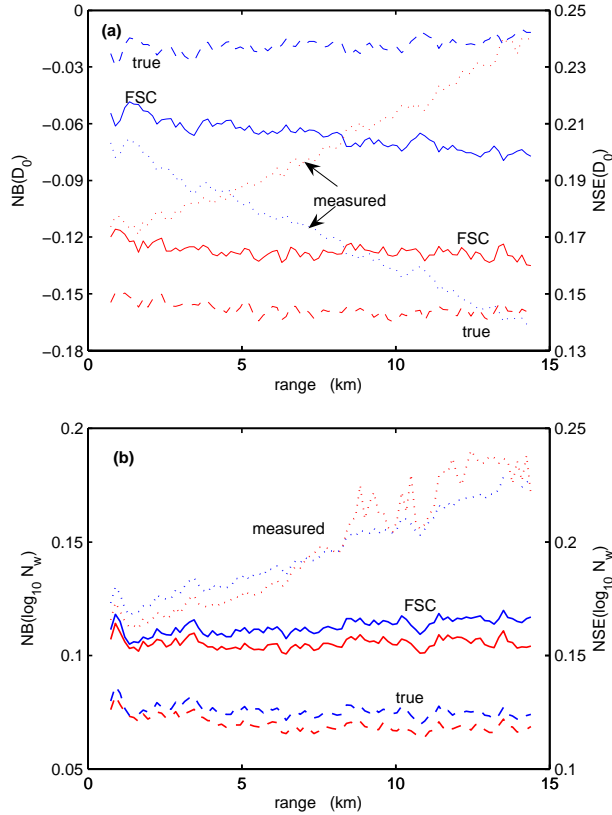


Fig. 2: The same of Fig. 1a and Fig. 1b for rain drops following the BC drop shape model

and 1700 UTC. Radar images of reflectivity showed a large radar echo composed of convective rain embedded in stratiform precipitation at the beginning of the rainstorm. Subsequently, the rainstorm evolved towards a more pronounced stratiform regime.

The test data were obtained from the range profiles with Z_h greater than 0 dBZ and power at the antenna greater than -110 dBm over at least 15 km of consecutive bins that presented an increase of Φ_{dp} greater than 3 degrees. Using these conditions, a data set of about 8500 profiles was built. Radar data consists of Z_h , Z_{dr} , and Φ_{dp} measurements, available every 150 m in range and obtained processing 256 samples. Differential phase profiles were filtered in range (Hubbert and Bringi 1995) to minimize the effects due to the phase shift on backscattering.

To estimate β , path-averaged value of Z_h , Z_{dr} and K_{dp} obtained as described in the previous section, are used to obtain pairs of K_{dp}/Z_h and Z_{dr} for each path. Fig. 3 shows the contours of the distribution of the K_{dp}/Z_h and Z_{dr} values. In the figure, as a reference, the behavior of the different averaged K_{dp}/Z_h path values as a function

of Z_{dr} obtained from simulations for different drop-shape models are also plotted. In particular, the linear models characterized by β equals to 0.04, 0.05, 0.062, and 0.07 mm⁻¹ (referred to as $\beta 4$, $\beta 5$, PB, $\beta 7$, respectively), and the non linear models by Beard and Chuang (1987), Andsager et al. (1999), Keenan et al. (2001), and Brandes et al. (2002) (referred to as BC, ABL, KZCM, BZV, respectively) are considered. Comparing the distribution of the K_{dp}/Z_h and Z_{dr} values with the corresponding values of the chosen models, a larger amount of information about the prevailing underlying drop shape model can be obtained. The contours of Fig. 3 are located essentially between the PB and BC lines. In particular, values of the ratio K_{dp}/Z_h as a function of Z_{dr} present values closer to the BC line and tend to approach the PB line with increasing Z_{dr} . In other words, raindrops show to become more oblate as Z_{dr} increases. An important point that needs to be highlighted is that the drops of the considered precipitation event present, on average, shapes that are more oblate than those described by the BZV, ABL and KCZM models. These findings appears in accordance with the results obtained by Gorgucci et al (2006b) using S-band measurements.

8. ACKNOWLEDGMENTS

This research was partially supported by the Italian Ministry of University and Research through the AEROCLOUDS project, by the National Science Foundation (ERC-0313747) and the NASA Precipitation Measurement Mission (TRMM/GPM) programs. Special thanks to Christian Kummerov for providing the X-Pol radar data and to Sergey Matrosov (CIRES/NOAA) for assistance with decoding the data.

9. REFERENCES

- Andsager, K., K. V. Beard, and N. F. Laird, 1999: Laboratory measurements of axis ratios for large raindrops. *J. Atmos. Sci.*, 56, 2673–2683.
- Beard K. V. and C. Chuang, 1987: A new model for the equilibrium shape of raindrops. *J. Atmos. Sci.*, 44, 1509–1524.
- Bringi, V. N., V. Chandrasekar, N. Balakrishnan and D. S. Zrnić, 1990: An Examination of Propagation Effects in Rainfall at Microwave Frequencies, *J. Atmos. Ocean. Tec.*, 7, 829–840.
- Bringi, V. N. and V. Chandrasekar, 2001: Polarimetric doppler weather radar: principles and applications. Cambridge University Press, 648 pp.
- Bringi, V.N., V. Chandrasekar, J. Hubbert, E. Gorgucci, W. L. Randeu and M. Schoenhuber, 2003: Raindrop size distribution in different climatic regimes from disdrometer and dual-polarized radar analysis. *J. Atmos. Sci.*, 60, 354–365.
- Brandes, E. A., G. Zhang, and J. Vivekanandan, 2002: Experiments in rainfall estimation with a polarimetric

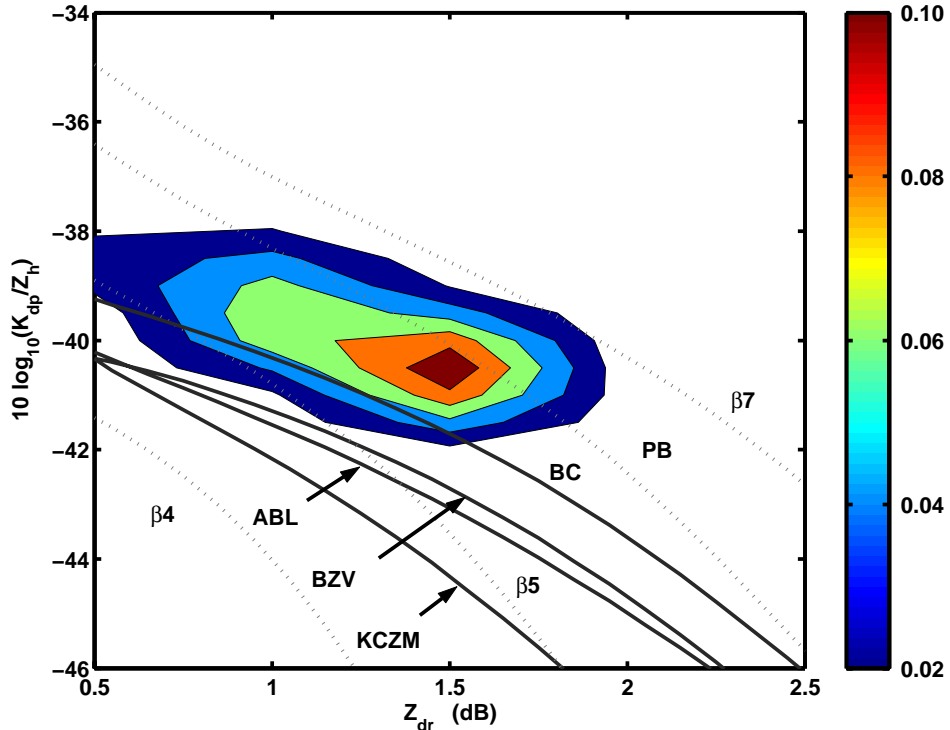


Fig. 3: Occurrence frequency of $(K_{dp}/Z_h, Z_{dr})$ pairs for NOAA ESRL X-POL data collected on 11 April 2001 during a campaign conducted at the NASA Wallops Island facility in Virginia. Averaged values for widely varying DSD obtained from the nonlinear shape-size relations of BC, ABL, KCZM, BZV (dark grey lines) and the linear relations of PB, $\beta=0.04 \text{ mm}^{-1}$, $\beta=0.05 \text{ mm}^{-1}$, $\beta=0.07 \text{ mm}^{-1}$ (light grey dot lines) are also shown.

- radar in a subtropical environment. *J. Appl. Meteor.*, **41**, 674–685.
- Brandes, E.A., G. Zhang and J. Vivekanandan, 2003: An evaluation of a drop distribution-based polarimetric radar rainfall estimator. *J. Appl. Meteor.*, **42**, 652–660.
- Chandrasekar, V., S. Lim, N. Bharadwaj, W. Li, D. McLaughlin, V. N. Bringi, and E. Gorgucci: 2004. Principles of networked weather radar operation at attenuating frequencies. *3rd European Conference on Radar in Meteorology and Hydrology*, Visby, Sweden, 67–73.
- Chandrasekar, V., S. Lim, and E. Gorgucci, 2006: Simulation of X-band rainfall observations from S-Band radar data. *J. Atmos. Oceanic Technol.*, **23**, 1195–1205.
- Gorgucci, E., G. Scarchilli, V. Chandrasekar and V. N. Bringi. 2000: Measurement of mean raindrop shape from polarimetric radar observations. *J. Atmos. Sci.*, **57**, 3406–3413.
- Gorgucci, E., V. Chandrasekar, V. N. Bringi, and G. Scarchilli, 2002: Estimation of raindrop size distribution parameters from polarimetric radar measurements. *J. Atmos. Sci.*, **59**, 2373–2384.
- Gorgucci, E., V. Chandrasekar, and L. Baldini, 2006a: Correction of X-band radar observation for propagation effects based on the self-consistency principle. *J. Atmos. Oceanic Technol.*, **23**, 1668–1681.
- Gorgucci, E., L. Baldini, and V. Chandrasekar 2006b: What is the shape of raindrops? An answer from radar measurements. *J. Atmos. Sci.*, **63**, 3033–3044.
- Gorgucci E. and L. Baldini, 2007: Attenuation and differential attenuation correction of C-band radar observations using a fully self-consistent methodology. *IEEE Geoscience and Remote Sensing Letters*, **4**, 326–330.
- Keenan, T. D., L. D. Carey, D. S. Zrnić and P. T. May. 2001: Sensitivity of 5-cm wavelength polarimetric radar variables to raindrop axial ratio and drop size distribution. *J. Appl. Meteor.*, **40**, pp. 526–545.
- Hubbert, J. and V.N. Bringi, 1995: An iterative filtering technique for the analysis of copolar differential phase

- and dual-frequency radar measurements. *J. Atmos. Oceanic Technol.*, **12**, 643–648.
- Illingworth, A. J. and T. M. Blackman, 2002: The need to represent raindrop size spectra as normalized gamma distributions for the interpretation of polarization radar observations. *J. Appl. Meteor.*, **41**, pp. 286–297.
- Martner, B. E., K. A. Clark, S. Y. Matrosov, W. C. Campbell, and J. S. Gibson, 2001: NOAA/ETL's polarization-upgraded X-band "HYDRO" radar. Preprints, 30th Int. Conf. on Radar Meteorology, Munich, Germany, Amer. Meteor. Soc., 101–103.
- Matrosov, S. Y., A. Clark, B. E. Martner, and A. Tokay, 2002: X-band polarimetric radar measurements of rainfall. *J. Appl. Meteor.*, **41**, 941–952.
- Moisseev, D. N., V. Chandrasekar, C. M. H. Unal and H. W. J. Russchenberg, 2006: Dual-polarization spectral analysis for retrieval of effective raindrop shapes. *Atmos. Oceanic Technol.*, **23**, 1682–1695.
- Pruppacher, H. R. and K.V. Beard, 1970: A wind tunnel investigation of the internal circulation and shape of water drops falling at terminal velocity in air. *Quart. J. Roy. Meteor. Soc.*, **96**, 247–256.
- Scarchilli G., E. Gorgucci, V. Chandrasekar, and A. Dobaie, 1996: Self-consistency of polarization diversity measurement of rainfall. *IEEE Trans. Geosci. Remote Sens.*, **34**, 22–26.
- Seliga, T.A., V. N. Bringi and H. H. Al-Khatib, 1981: A preliminary study of comparative measurement of rainfall rate using the differential reflectivity radar technique and a raingauge network. *J. Appl. Meteorol.*, **20**, 1362–1368.
- Testud, J., E. Le Bouar, E. Obligis, and M. Ali-Mehenni, 2000: The rain profiling algorithm applied to polarimetric weather radar. *J. Atmos. Oceanic Technol.*, **17**, 332–356.
- Ulbrich, C., 1983: Natural variations in the analytical form of the raindrop-size distribution. *J. Climate Appl. Meteor.*, **22**, 1764–1775.